Spectroscopy of high *n* Rydberg states of the triatomic deuterium molecule D_3

U. Müller, U. Majer, R. Reichle, and M. Braun
Universität Freiburg, Fakultät für Physik, Hermann-Herder-Str. 3, D-79104 Freiburg, Germany

(Received 8 January 1997; accepted 11 February 1997)

We report first investigations of high principal quantum number Rydberg states of the neutral triatomic deuterium molecule. The experiments were performed using a fast neutral beam photoionization spectrometer recently developed at Freiburg. A fast beam of metastable D_3 molecules was created by charge transfer of a D_3^+ beam in cesium. Rydberg states of D_3 were analyzed by pulsed-laser excitation using two-photon resonance-enhanced ionization, electric field ionization and autoionization. Our data identify the $2p\ ^2A_2''(N=K=0)$ state of D_3 to be metastable with a lifetime of about 1 μs. The spectral lines following excitation in the ultraviolet spectral range were assigned to *s*-type and *d*-type Rydberg-series converging to vibrational ground state, symmetric stretch excited and degenerate mode excited D_3^+ ion states. By a combination of vibrationally diagonal and non-diagonal transitions, we determined the ionization potential, the symmetric stretch and degenerate mode vibrational frequencies of the $2p\ ^2A_2''$ state in D_3. The data give insight into the influence of the coupling between the Rydberg electron and the ion core on the potential energy surface. © *1997 American Institute of Physics.* [S0021-9606(97)00819-2]

I. INTRODUCTION

The H_3 molecule, the simplest neutral polyatomic molecule, plays an important role in molecular physics. The system is ideally suited to study fundamental aspects of the electron–core interaction and it is sufficiently small for successful *ab initio* investigations. The H_3 molecule is also important for applications in hydrogen plasmas and in astrophysics. While the ground state of H_3 is repulsive, excited states exist which can be regarded as Rydberg states with a tightly bound H_3^+ core. They were first discovered by Herzberg and coworkers[1–4] in emission from an electrical gas discharge in hydrogen. Devienne,[5] Gellene and Porter[6] and Garvey and Kuppermann[7] found evidence for the existence of a metastable state of H_3 in fast neutral beams created by charge transfer of H_3^+. The $2p\ ^2A_2''(N=K=0)$ state is the only metastable state of H_3 (Ref. 8) and was used as a platform for laser-excitation/ionization experiments which give insight into the level structure and the dynamics of H_3 as well as that of H_3^+. Photoexcitation into *s*- and *d*-type Rydberg series[9–13] was used to determine the vibrational frequencies of the $2p\ ^2A_2''(N=K=0)$ metastable state of H_3 as well as the symmetric stretch frequency of H_3^+. Experiments involving two-step laser-excitation processes were required in order to measure the symmetric stretch vibrational frequencies of the low principal quantum number Rydberg states[8,14,15] and to investigate *p*- and *f*-type Rydberg series which are not accessible by single photon absorption from the $2p\ ^2A_2''$ state.[16,17] All of the excited states of H_3 are embedded in the continuum of the repulsive ground state. Therefore, the lifetime of Rydberg states[18] is strongly influenced by predissociation due to coupling with the ground state. Several window resonances were discovered in the Rydberg series of H_3 (see Ref. 18 and references therein) and interpreted by the electron–core interaction due to mixing with neighboring states of different core excitation which are strongly predissociated. The nature of many of these window resonances is still unexplained.

The potential energy surfaces of the lowest Rydberg states $2s\ ^2A_1'$, and $2p\ ^2A_2''$ of H_3 were studied recently in an *ab initio* investigation by Peng *et al.*[19] By using different isotopes, the density and the location of the vibrational and rotational levels is changed with the electronic states remaining almost at the same energetic places. Thus, different regions of the potential energy surface are probed in D_3 and H_3 experiments. The electron–core coupling is also affected by the nuclear mass and can be studied in a comparison between different isotopomers.

Little is known about the vibrational spacings in the Rydberg states of D_3. Some of them have been derived from vibrationally non-diagonal emission bands but the uncertainty was of the order of 10 cm^{-1} due to an unresolved rotational structure.[20,21] The aim of our study is to spectroscopically identify the metastable states of D_3 and to measure the ionization potentials and the vibrational frequencies.

II. EXPERIMENT

A new fast beam collinear spectrometer recently developed at Freiburg was first employed in the study reported here. A schematic diagram of the apparatus which is similar to the setup at SRI-International[9,10,13] is presented in Fig. 1.

D_3^+-ions are created by the ion–molecule reaction,

$$D_2^+ + D_2 \rightarrow D_3^+ + D, \tag{1}$$

in a hollow cathode discharge source. The length of the cathode was 1.5 cm and the diameter was 1.2 cm. The source was operated at a pressure of about 1 mbar (10^{+2} Pa) and the cathode was cooled by liquid nitrogen in order to produce rotationally and vibrationally cold D_3^+-ions. At these operating conditions, the ratio of D_2^+ to D_3^+ ion current was found

 0021-9606/97/106(19)/7958/10/$10.00

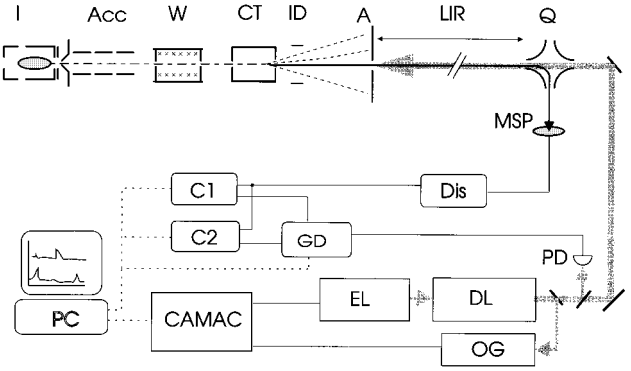

FIG. 1. Schematic of the Freiburg neutral beam photoionization spectrometer. Legend: I: hollow cathode discharge ion source; Acc: ion beam extraction and acceleration stage; W: Wien filter; CT: charge transfer cell; ID: ion deflector; A: aperture; LIR: laser interaction region; Q: electric quadrupole ion deflector; MSP: microsphere plate detector; Dis: discriminator; C1, C2, GD: dual 200 MHz counter with programmable gate and delay generator; EL: XeCl excimer laser; DL: pulsed dye laser; OG: optogalvanic reference cell; PD: photodiode; CAMAC: digital and analog data transfer to and from laboratory computer based on CAMAC.

to be of the order of 1:10. The ions were extracted through an aperture of 0.2 mm in diameter, and accelerated to an energy of 3.6 keV. A mass selection was performed using a Wien-filter. A small fraction of the D_3^+-ions was neutralized by charge transfer in cesium vapor. After the charge-transfer cell, the unreacted ions were removed by an electric field. A 1 mm diameter aperture (AP) located 30 cm downstream of the charge transfer cell was used to stop products of dissociative charge transfer and to allow a beam of metastable D_3 molecules to enter the 120 cm long laser-interaction region. The photoexcitation or photoionization was performed by a pulsed dye-laser beam. At the end of the interaction region, D_3^+ photoions are detected by an energy analyzer (electric quadrupole deflector) and a microsphere plate (El Mul) connected to a fast discriminator (Ortec, Mod. 9302). Molecules which are excited to high principal quantum number Rydberg states are field-ionized in the electric field of the quadrupole deflector and can also be detected. Photoions and ions from electric field-ionization of high Rydberg states can be distinguished by applying a small electric field perpendicular to the flight path in the interaction region.

Since the velocity of the metastables in the neutral beam is about 1% of the speed of light, the photoions arrive at the detector in a time window of several μs after the 10–15 ns wide laser pulse. The events were monitored by a synchronized, gated 200 MHz dual-counter (SRS, Mod. SR400). One of the counter channels (day-channel) was gated for the detection of photoexcitation-events created along the 120 cm interaction region during the laser pulse. The gate of the second channel was delayed sufficiently to register background events only (night-channel). The events in the day- and night-channels were accumulated for a preselected number (100 to 500) of laser shots. The data were then transferred to a laboratory computer and stored for further treatment. The background signal is typically 5×10^{-3} ions per μs. Photoexcitation signals as low as 10^{-2} events per laser shot are readily detected. The dye-laser (Scanmate 1, Lambda-Physik) was pumped by an Excimer-laser (LPX110, Lambda-Physik) operating at 308 nm (XeCl). The wavelength scan of the dye-laser was performed under control of the laboratory computer. A small portion of the laser light was directed into a hollow cathode discharge in neon or argon. The optogalvanic signal[22] was recorded by the laboratory computer and provided a reference spectrum of atomic lines. From the optogalvanic spectrum, we estimate the laser bandwidth to be less than 6 pm at 588 nm and 2.7 pm at 340 nm. After application of a linear correction to the laser wavelength scale, the measured optogalvanic lines coincided with the tabulated values[23] within 2 pm. The Rank-formula[24] was used to correct for the refractive index of air. The Doppler-shift due to the motion of the fast neutral molecules was calculated from the acceleration voltage of the ion source. In order to test the accuracy of the calibration procedure, we generated a fast beam of atomic hydrogen in the $2s$ state by charge transfer of protons in cesium. We observed the np Rydberg series by field-ionization following laser-excitation from the $2s$ state. The series limit observed by us coincides within 0.15 cm^{-1} with the well-known ionization energy of the H($2s$) state of atomic hydrogen, 27419.816 cm^{-1}.[25]

The number of ion events at the detector depends on the density of the metastable beam, the laser intensity, the transition matrix element and the ionization efficiency by the photo-, field- or autoionization process. The laser energy is not depleted by the low molecular density in the neutral beam. In the case of a collimated laser beam, the number of photoions or photoexcited molecules for a specific transition is proportional to the population of the metastable state. The duration of the laser pulse is short compared to the propagation time of the heavy particles along the interaction region. In the absence of any loss mechanism of the excited state population, the arrival time spectrum of the photoions reflects the distribution of excitable molecules along the laser interaction region. This allows us to determine the lifetime of the metastable state. For the time-of-flight measurements, we used a fast multistop time-to-digital converter (Fast-CMTE, Mod. 7885) with a resolution of 5 ns which was started by the signal of the photodiode and stopped by the pulses from the ion detector. The spectrum was accumulated in a histogramming memory (FAST Comtec MCD/PC) which was connected to the laboratory computer.

III. RESULTS AND DISCUSSION

A. Identification of the metastable state in D_3

The H_3 molecule was discovered by Dabrowski and Herzberg[1] from emission bands of the $3s\ ^2A_1'\rightarrow 2p\ ^2A_2''$ and $3p\ ^2A_2''\rightarrow 2s\ ^2A_1'$ transitions. The lines observed in these bands are remarkably broad due to predissociation of the $2s\ ^2A_1'$ and $2p\ ^2A_2''$ lower states by coupling with the repulsive $2p\ ^2E'$ ground state potential energy surface. Predissociation of a ns^2A_1' Rydberg level is mediated by vibronic coupling to the $2p\ ^2E'$ state via the degenerate mode vibration (symmetry species E'). The coupling strength depends on the Franck–Condon overlap which decreases for higher

principal quantum numbers. The lifetime of the $2s\ ^2A_1'$ state is reduced to 150 femtoseconds by predissociation.[18] By contrast, the $3s\ ^2A_1'$ state lives sufficiently long to be observed in emission. The $2p_z$ state has $^2A_2''$ electronic symmetry and cannot couple to the $2p\ ^2E'$ state by a normal vibration. In this case, predissociation is mediated by rotation about an axis perpendicular to the symmetry axis. Therefore, the observed linewidth in the $3d\ ^2E''-2p\ ^2A_2''$ band in H_3 was found to increase proportional to $N(N+1)-K^2$, where N and K are the quantum numbers of the total angular momentum apart from spin and of the projection onto the C_3 axis, respectively.[1,4] As a consequence, the $2p\ ^2A_2''(N=K=0)$ state in H_3 is immune against predissociation even with a symmetric stretch or degenerate mode vibration excited.[8] It may slowly decay by radiation into the $2s\ ^2A_1'$ state which lies 898 cm^{-1} lower in energy. From the transition moment calculated by King and Morokuma[26] and by Petsalakis *et al.*,[27] a lifetime of about 80 μs would result.[6] The observed lifetime of 640 ns[28] is much shorter than this value. Bjerre *et al.*[29] found that the observed decay rate cannot be explained by predissociation due to spin–orbit coupling. A radiative decay into the unstable $2p\ ^2E'$ state combined with excitation of a quantum in the degenerate vibrational mode was invoked to explain the observed lifetime.[28] This explanation is consistent with the kinetic energy release spectrum of the $H+H_2$ fragments following decay of the $2p\ ^2A_2''$ state observed by Cosby and Helm[30] and by Müller and Cosby.[31] The $2p\ ^2A_2''(N=K=0)$ state of H_3 can be viewed as a $2p_z$ Rydberg electron attached to a $H_3^+(N^+=1,\ K^+=0)$ core. Since the $N^+=0,\ K^+=0$ level does not exist in H_3^+ due to proton spin statistics,[32] the $N^+=1,\ K^+=0$ state is the lowest *ortho*-level of H_3^+ and is highly populated in a cold ion source. Therefore, a fast beam of $H_3\ 2p\ ^2A_2''$ molecules in the single rotational state $(N=K=0)$can be generated very efficiently by near-resonant charge transfer of H_3^+ in cesium. Molecules in the $2s\ ^2A_1'$ state or in rotationally excited levels of the $2p\ ^2A_2''$ state are subject to predissociation with appreciable kinetic energy release. The fragments are removed from the neutral beam by the aperture A in Fig. 1. Rydberg states with $n\geqslant 3$ are connected by radiative transitions to the $2s\ ^2A_1'$, $2p\ ^2A_2''$, or $2p\ ^2E'$ states. In addition, they are also subject to predissociation. The lifetimes of the $n=3$ Rydberg states were observed to be of the order of a few nanoseconds[20,21,33] which is short compared to the flight time of the neutral beam between the charge transfer cell and the aperture A. Contributions from very high n Rydberg states of H_3 in the neutral beam can be quenched by the deflection field after the charge transfer cell.

The considerations above concerning the electronic eigenstates, the optically allowed transitions and the coupling mechanisms remain in principle valid when the protons in the H_3^+ core are replaced by deuterons, except for the following details which make the experimental investigations more difficult. In the case of deuterons, the total wavefunction including nuclear spin has to be symmetric with respect to interchange of two identical nuclei (Bose statistics). In a totally symmetric electronic and vibrational state, the statistical weight of rotational levels with $K=0$ alternates by a ratio of 10:1 between even and odd values of N (Ref. 34, p. 28). As a consequence, the $N^+=1,\ K^+=0$ level in D_3^+ which is required to build the $D_3\ 2p\ ^2A_2''(N=K=0)$ state is much less populated than the corresponding ionic core state in H_3^+. Indeed, we find the beam of $2p\ ^2A_2''(N=K=0)$ metastables to be by one order of magnitude weaker for D_3 than for H_3 at similar ion source conditions. This is in agreement with the observations by Gellene and Porter.[6]

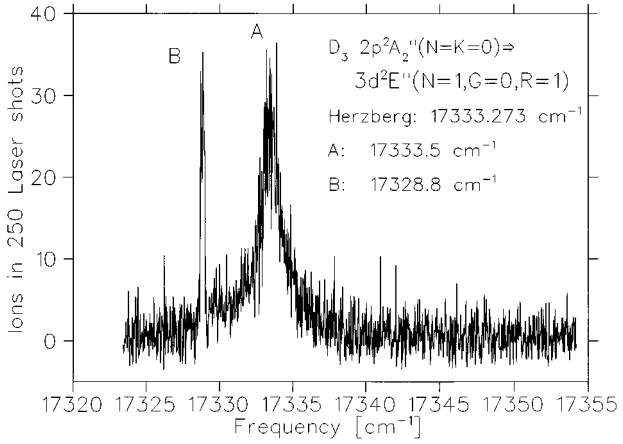

FIG. 2. Two-photon ionization spectrum of metastable D_3 molecules in the 17320 cm^{-1} to 17355 cm^{-1} photon energy range. Peak A is due to the $2p\ ^2A_2''(N=K=0)\rightarrow 3d\ ^2E''(N=1,\ G=0,\ R=1)$ transition observed in emission at 17333.273 cm^{-1} by Herzberg *et al.*[4]

The Rydberg states are embedded in but do not cross the ground state potential energy surface. Since the width of the vibrational wavefunction decreases at higher nuclear masses, the Franck–Condon overlap which governs the strength of the vibrational coupling is expected to be smaller in D_3 than in H_3. The lines of the $3d\ ^2E''\rightarrow 2s\ ^2A_1'$ transition were observed to be much sharper in D_3 than in H_3.[1] The rotational coupling is less effective in H_3 than it is in D_3. In the emission study of the $3d\ ^2E''\rightarrow 2p\ ^2A_2''$ transition in D_3, the linewidth was observed to be practically independent of N and K.[1] In our present setup, a molecular state has to survive the travel between the charge transfer cell and the aperture A in order to be available for the laser-excitation process. As a consequence, its lifetime has to be of the order of one hundred nanoseconds or longer. It is unlikely that the lifetimes of $2p\ ^2A_2''$ states with $N>0$ which for H_3 were observed to be in the picosecond range[18] increase by five orders of magnitude in the case of D_3. Hence, we expect our spectra to arise only from molecules in the metastable $N=K=0$ rotational level. In the following, we discuss the identification of the lower state in our photoexcitation study.

In Fig. 2, the two-step photoionization spectrum of long-lived D_3 molecules formed by charge transfer of D_3^+ in cesium is presented in the 17320 cm^{-1} to 17355 cm^{-1} energy range. The Doppler-shift due to the motion of the target in the laboratory system was corrected for the counter-propagating laser and neutral beams. Two pronounced peaks

appear in this spectrum. The position of peak A at 17333.5 cm^{-1} agrees within the uncertainty of our wavelength calibration with the transition between the $2p\ ^2A_2''(N=K=0)$ and the $3d\ ^2E''(N=1,\ G=0,\ R=1)$ states in D_3 as observed in emission at 17333.273 cm^{-1} by Herzberg *et al.*[4] We interpret this as a proof for the existence of the $2p\ ^2A_2''(N=K=0)$ state in our neutral D_3-beam. The $3d\ ^2E''(N=1,\ G=0,\ R=1)$ upper state is sufficiently long-lived to be ionized by a second photon from the same laser pulse and can therefore be detected in our apparatus. According to the *ab initio* calculation by King and Morokuma,[26] the dipole moment of the $2p\ ^2A_2''\rightarrow 3d\ ^2E''$ transition is 8.15 a.u. which is comparatively large. At a pulse energy of 2 mJ of our laser, the excitation step is saturated which leads to a power-broadening. This explains the comparatively large linewidth of about 1.5 cm^{-1} FWHM observed for peak A in Fig. 2. The peak height is mainly determined by the ionization probability of the excited state and we observed it to scale almost linearly with the laser pulse energy.

The assignment of the narrow peak B in Fig. 2 at 17328.8 cm^{-1} is not clear at the moment. An experimental artifact due to laser-light scattered into the backward direction from the aperture behind the charge-transfer cell exciting the $2p\ ^2A_2''(N=K=0)\rightarrow 3d\ ^2E''(N=1,\ G=0,\ R=1)$ transition should appear Doppler-shifted to the high-energy side of peak A and therefore can be excluded. In the optogalvanic spectra, no indication was found for a multifrequency operation of the dye-laser. Peak B could be either a transition starting from a vibrationally excited $2p\ ^2A_2''$ metastable state or a non-resonant two-photon transition from the $2p\ ^2A_2''$ vibrational ground state into an autoionizing vibrationally core excited Rydberg state. We observed that Peak B scales quadratically with the laser power which favors the second explanation. For a systematic investigation and final assignment, the excitation and the ionization photon must be provided by separately tunable synchronously pumped dye-lasers.

B. Photoexcitation of high Rydberg states of D_3 in vibrationally diagonal series

In Fig. 3, the photoexcitation/ionization spectrum of the $D_3\ 2p\ ^2A_2''$ molecule between 27750 cm^{-1} and 29610 cm^{-1} is presented. In the 28920 cm^{-1} to 29610 cm^{-1} frequency range, the dye PTP was used and in the frequency range below 28920 cm^{-1} the dye DMQ was used. Most of the lines can be assigned to one of five different Rydberg series which are marked by the tick spectra labelled 1 to 5 in Fig. 3. The line positions were fitted by the Rydberg formula,

$$E(n)=E_{lim}-\frac{R_y}{(n-\delta)^2}, \tag{2}$$

with $R_y=109727.353$ cm^{-1} the Rydberg constant for triatomic deuterium. The series limits E_{lim} and the quantum defects δ of the five series are listed in Table I along with the range of principal quantum numbers observed and used in the fit. The residuals of the five series are presented in Fig. 4. For quantum numbers above $n=14$, the observed and fitted line positions generally agree within the systematic uncertainty of our wavelength calibration. At lower principal quantum numbers, deviations from equation (2) smaller than 2 cm^{-1} are observed. Series 1 and 2 and series 3 and 4 converge to the same series limits of 29601.0 cm^{-1} and 29535.1 cm^{-1}, respectively. Series 5 converges to a limit of 29547.8 cm^{-1}. When comparing these values to the lowest ionization limit of the $2p\ ^2A_2''(N=K=0)$ ground vibrational state of H_3, 29562.14 cm^{-1},[12] we find the difference to be by one order of magnitude smaller than the ν_2 vibrational spacing in D_3^+. We conclude that all series marked in Fig. 3 must be vibrationally diagonal transitions. Franck–Condon factors for the excitation of vibrationally non-diagonal transitions are very small since the rotational constants B_0 and thus the internuclear separations are very similar in the $2p\ ^2A_2''$ state of D_3 ($B_0=22.1089$ cm^{-1} [3]) and in the ground state of D_3^+ ($B_0=21.810$ cm^{-1} [35]). We do not find any indication for a rotational structure in the observed spectra. Therefore, the $D_3\ 2p\ ^2A_2''$ lower state must be in the lowest rotational level $(N=K=0)$ which can only be excited by R-branch transitions into $ns\ ^2A_1'(N=1,K=0)$ and $nd\ ^2A_1'(N=1,K=0)$ Rydberg states according to the selection rule $\Delta K=0$, $\Delta N=\pm 1$ for parallel transitions.[1]

By applying a small electric field in the interaction region perpendicular to the neutral beam direction, the lines of series 3, 4 and 5 are observed to disappear while the intensities of the lines belonging to series 1 remain almost unaffected. This shows that the upper states of series 1 are field-ionized in the detector and thus converge to the ground vibrational state of D_3^+. Series 3 to 5 result from autoionizing states with vibrationally excited D_3^+ cores. Therefore, series 1 and 2 are assigned to transitions starting in the ground vibrational $2p\ ^2A_2''$ state. This is in line with the observation that series 1 reveals by far the highest intensity. Since the source was cooled to liquid nitrogen temperature, we expect the ground vibrational level to be the most populated level in the D_3^+ beam. The vibrational population is not expected to be modified significantly in a near-resonant charge transfer process.

The fit to the line positions of series 1 between $n=20$ and $n=80$ by the Rydberg formula 2 requires a quantum defect of 0.016. The lines of series 2 which are by one order of magnitude weaker than those of series 1, are clearly separated in the spectrum Fig. 3 in the $n=22$ to $n=31$ range but blend with lines of series 1 at higher n values. The quantum defect of series 2 was found to be 0.08. In the hydrogen atom, the dipole moment for transitions from the $2p$ state into the nd series is by a factor of about 16 higher than that into the ns series at high principal quantum numbers (Ref. 36, p. 264). Therefore, we assign series 1 to the transition from the vibrationless $2p\ ^2A_2''(0,0,0,0)$ state into vibrationless $nd\ ^2A_1'(0,0,1,0)$ Rydberg states and the lines of series 2 to the corresponding transitions into the $ns\ ^2A_1'(0,0,1,0)$ Rydberg states. Here, the rovibrational states were labelled by the quantum numbers $(\nu_1,\ \nu_2,\ N,K)$. The observed quantum defect of the $nd1$-series is very similar to the value of 0.0189 observed for the corresponding series in H_3.[10] The vibrationless $ns1$-series was not observed in H_3. Apparently, due to

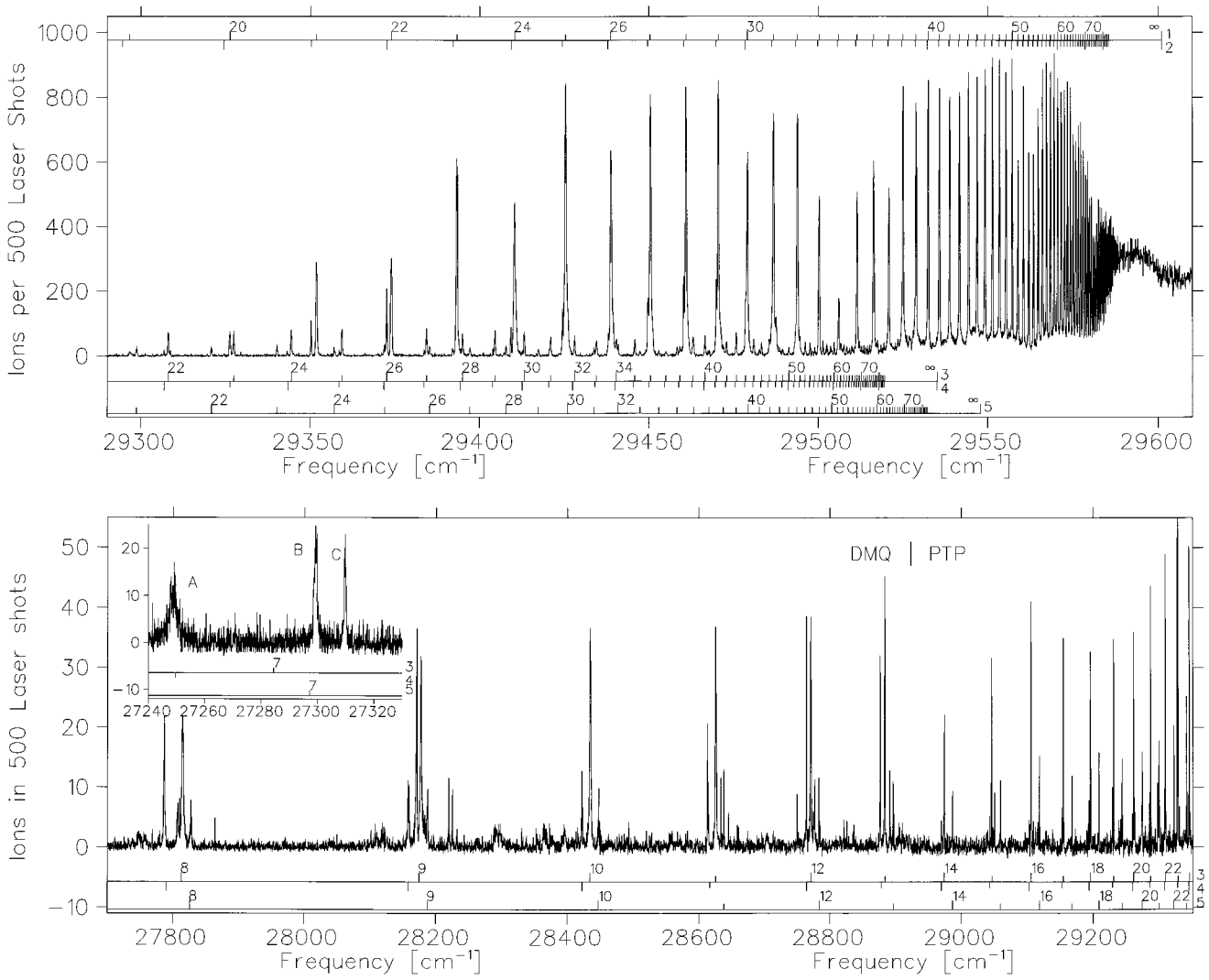

FIG. 3. Spectrum of field-ionizing and autoionizing lines following laser-photoexcitation of D_3 $2p\ ^2A_2''$ molecules in the ultraviolet range between 27750 cm^{-1} and 29610 cm^{-1}. Most of the lines can be assigned to one of the five Rydberg series indicated by the tick spectra in the figure. The spectral range between 27240 cm^{-1} and 27330 cm^{-1} is included as an inset. In the 28920 cm^{-1} to 29610 cm^{-1} frequency range, the dye PTP was used and in the frequency range below 28920 cm^{-1} the dye DMQ was used.

predissociation the lifetime of the lower *n* states of the $ns1$-series in H_3 is shorter than the travel time along the laser-interaction region. The larger quantum defect of the *s*-series compared to that of the *d*-series can be understood by the higher overlap of the electronic wavefunction with the

TABLE I. Rydberg series observed following laser-photoexcitation of metastable D_3 $2p\ ^2A_2''$ molecules.

No.	E_{lim} (cm^{-1})[a]	δ	Observed *n*	$^2A_2''$ [b]	Upper state [b]
1	29601.0	0.015(8)	20–80	(0,0,0,0)	$nd1$ (0,0,1,0)
2	29601.0	0.08(1)	22–31	(0,0,0,0)	$ns1$ (0,0,1,0)
3	29535.1	0.014(1)	8–71	(0,1,0,0)	$nd1$ (0,1,1,0)
4	29535.1	0.07(6)	8–31	(0,1,0,0)	$ns1$ (0,1,1,0)
5	29547.8	0.015(1)	7–46	(1,0,0,0)	$nd1$ (1,0,1,0)

[a]The statistical uncertainty of the fit procedure is smaller than the 0.2 cm^{-1} systematic uncertainty of the wavelength calibration.
[b]The notation for the rovibrational state is (ν_1, ν_2, N, K).

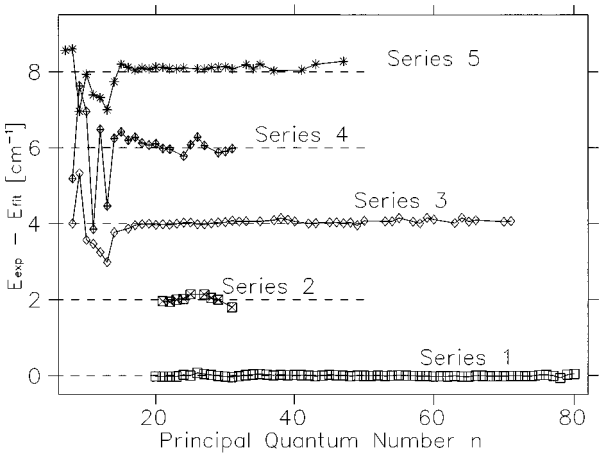

FIG. 4. The difference between the observed line positions and the fit by the Rydberg formula for series 1 to 5 listed in Table I. The zerolines for the individual series indicated by the dashed lines are shifted with respect to each other for clarity of presentation.

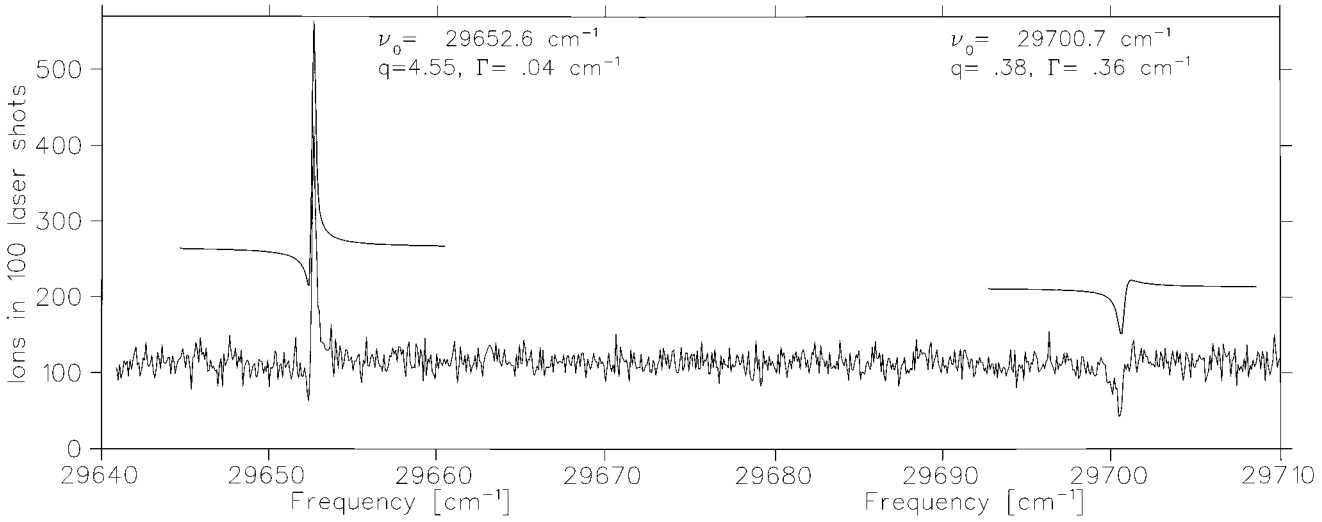

FIG. 5. Photoionization spectrum of D_3 $2p\ ^2A_2''$ molecules in the 29640 cm^{-1} to 29710 cm^{-1} energy range.

ion core leading to a higher effective charge. By similar considerations, series 3 and 4, which have quantum defects of 0.014 and 0.08, respectively, are assigned to *nd* and *ns* Rydberg series converging to a vibrationally excited D_3^+ core. The lines of series 5, which are weaker than those of series 3, can be fitted with a quantum defect of 0.015 which makes an assignment to a *nd* series very probable. There are indications for the existence of a corresponding *ns* series, but their intensities are too small to make a clear statement.

The assignment of the core vibrational excitation of series 3 to 5 can be performed based on the lowest principal quantum number lines observed in the spectra. Since Rydberg states with principal quantum numbers below $n=20$ cannot be field-ionized in the quadrupole deflector, low-*n* Rydberg states can only be detected by autoionization in the case of a single-photon excitation process. The rovibrational levels of D_3^+ are very well known. The vibrational sequence of the degenerate mode (ν_2) was measured and the vibrational and rotational constants of the symmetric stretch sequence (ν_1) were predicted by Amano *et al.*[35] using the *ab-initio* potential energy surface by Meyer, Botschwina and Burton.[38] This allows us to calculate the energy $E^+(\nu_1,\nu_2)$ of the $D_3^+(\nu_1,\nu_2,N^+=1,K^+=0)$ ion core above the $D_3^+(0,0,0,0)$ state listed in column 2 of Table III. The minimum effective principal quantum number $(n-\delta)$ required for vibrational autoionization which is listed in column 3 of Table III was calculated from the energy difference $E^+(\nu_1,\nu_2) - E^+(0,0)$ using the Rydberg-formula (2). We find no indication for lines with $n=6$ in the observed spectra which restricts the possible core states of series 3 to 5 to the lowest vibrational states ($\nu_1=0$, $\nu_2=1$) and ($\nu_1=1$, $\nu_2=0$). This is in line with the low vibrational temperature of the D_3^+ ions in the primary beam which is expected not to be changed by the near-resonant charge transfer process. According to Table III, the autoionizing lines of the $ns1$- and $nd1$-series built on ($\nu_1=1$, $\nu_2=0$) and ($\nu_1=0$, $\nu_2=1$) cores are restricted to $n\geqslant 7$ and $n\geqslant 8$, respectively. The inset in Fig. 3 shows the photoionization spectrum in the 27240 cm^{-1} to 27330 cm^{-1} energy range. We observe three peaks, labelled A to C. Any peak in this spectral range resulting from a vibrationally diagonal transition must be due to a $n=7$ upper state. None of the peaks in Fig. 3 can be assigned to series 3. The position of peak B is in excellent agreement with the prediction of series 5 for $n=7$ with a residual less than 0.3 cm^{-1}. This leads us to conclude that series 3 and 5 are $nd1$ series with ($\nu_1=0$, $\nu_2=1$) and ($\nu_1=1$, $\nu_2=0$) core vibrational excitation, respectively. Series 4 is assigned to the $ns1$-series with a ($\nu_1=1$, $\nu_2=0$) core. Our assignment is supported by preliminary results of a two-photon depletion experiment which shows that the peaks A, B, C and the $n=8$ peak of series 5 originate from the same lower state. The quantum defects of peaks A and C calculated from the 29547.8 cm^{-1} limit of the $nd1$- ($\nu_1=1$, $\nu_2=0$) series are 0.09 and -0.002, respectively. Peak A results most likely from the $7s1$ ($\nu_1=1$, $\nu_2=0$) state. Peak C could be an interloper state from the *g*-series. The final assignment is not possible at present and requires further investigation by two-photon excitation/depletion experiments.

C. Vibrationally non-diagonal transitions

The photoionization spectrum of metastable D_3 molecules in the 29640 cm^{-1} to 29710 cm^{-1} photon energy range is shown in Fig. 5. This spectral range lies in the continuum of the five Rydberg series discussed above. Two features labelled by A and B are observed in the spectrum. The asymmetric line-profiles are typical for interference in excitation to the discrete autoionizing states and the ionization continuum. The line shapes were fitted by Fano-type profiles,[39]

$$I(\epsilon)=I_0\cdot\left((1-\alpha)+\alpha\cdot\frac{(q+\epsilon)^2}{1+\epsilon^2}\right). \tag{3}$$

The reduced energy variable ϵ,

$$\epsilon=(E-E_0)/(\Gamma/2), \tag{4}$$

TABLE II. Fano profile parameters of the features observed in the ionization continuum following vibrationally non-diagonal excitation of D_3 $2p\ ^2A_2''$ molecules. The Fano-profiles were convoluted with a Gaussian apparatus profile of FWHM=0.2 cm^{-1} in width.

Feature	E_0 (cm^{-1})[a]	α [b]	q [c]	$\Gamma/2$ (cm^{-1})[d]	upper state[e]
A	29652.6	0.88	4.55	0.018	$7d1(1,0,1,0)$
B	29700.7	0.64	0.38	0.18	$8p1(0,1,1,0)$

[a]Line center including unobservable line shift due to interaction with continuum (cf. Fano[39]).
[b]Fraction of continuum interacting with the autoionizing state.
[c]Line shape parameter.
[d]Linewidth of autoionizing state.
[e]Lower state of both features is $2p\ ^2A_2''(0,0,0,0)$.

contains the photon energy E, the line-width Γ and the position of the resonance E_0. The slight shift between the unperturbed state and the center of the resonance discussed by Fano[39] cannot be determined experimentally and is incorporated in E_0. We introduced an additional parameter α which allows for an incoherent admixture of continua excited from other lower state levels which do not interfere with the autoionizing state. The parameter q describes the ratio of the transition probabilities to the discrete and the continuous states. In order to take the finite spectral resolution into account, a convolution with a Gaussian line profile was performed. This inhomogeneous linewidth, comprising the laser bandwidth and the Doppler broadening due to the finite neutral beam divergence, was estimated to be 0.2 cm^{-1} FWHM from the high principal quantum number lines of the field-ionizing series. The values of the fitted parameters E_0, α, q, and Γ are listed in Table II. The location of the feature E_0 turns out to be quite insensitive to a variation in the selected width of the apparatus function whereas the parameters α, q, and Γ may be influenced by as much as $\pm 50\%$. Despite the large systematic uncertainty, the values are still good enough for the following considerations.

The comparatively large values of α suggest that the lower state of both features is the $2p\ ^2A_2''(0,0,0,0)$ vibrational ground state which constitutes the majority in the neutral beam. Assuming the upper state to be a Rydberg state with a $(\nu_1,\nu_2,1,0)$ ion core, we can determine the principal quantum number n and the quantum defect δ of a feature located at E_f from the 29601.0 cm^{-1} first ionization limit of the $2p\ ^2A_2''(0,0,0,0)$ state (Table I) and the ion core energies $E^+(\nu_1,\nu_2,1,0)$ listed in column 2 of Table III according to the formula

$$E_f = E_{lim}(0,0,1,0) + E^+(\nu_1,\nu_2,1,0) - E^+(0,0,1,0) - R_y/(n-\delta)^2. \quad (5)$$

The results are listed for peak A at $E_f = 29652.6$ cm^{-1} in columns 4 and 5 and for peak B at $E_f = 29700.7$ cm^{-1} in columns 6 and 7 of Table III. Since the Franck–Condon factors for vibrationally non-diagonal transitions are rapidly decreasing with increasing difference in vibrational excitation, we expect the upper states to have at most one quantum of vibrational core excitation. In the case of H_3, the quantum defects of series converging to a $N^+=1,K^+=0$ excited core state have been observed to be close to zero,[10,12,16,17] except for the $np1A_2''$ series where a quantum defect of 0.39 was observed.[17] There is no reason for this tendency to change in the deuterated species. Therefore, the only reasonable assignment for Peak A is an $n=7$ upper state with a $(\nu_1=1, \nu_2=0)$ core. For the electronic wavefunction, we have the choice between an *s*- and a *d*-type orbital. If Peak A in Fig. 5 would belong to the *s*-series, we would expect a corresponding peak of the *d*-series about 30 cm^{-1} higher in frequency and by one order of magnitude stronger in intensity which is not observed. Thus, we assign Peak A in Fig. 5 to the $D_3\ \ 2p\ ^2A_2''(0,0,0,0) \rightarrow 7d1\ (1,0,1,0)$ transition.

For peak B at 29700.7 cm^{-1} the most reasonable choice is $(\nu_1=0,\ \nu_2=1)$ with $n=8$ and a quantum defect of $\delta=0.05$. Since the excitation of degenerate mode vibration consumes angular momentum from the photon field, the upper state electronic wavefunction must be a *p*-type orbital. For peaks A and B, the parameters q- and Γ differ by about one order of magnitude which is indicative of completely different excitation mechanisms. According to Fano,[39] the ratio between the transition probabilities into the discrete autoionizing state $|\langle\Phi|T|i\rangle|^2$ and the continuum $|\langle\Psi_E|T|i\rangle|^2$,

$$|\langle\Phi|T|i\rangle|^2/|\langle\Psi_E|T|i\rangle|^2 = \frac{1}{2}\pi q^2\Gamma, \quad (6)$$

can be expressed by q and Γ according to equation (6). Both features in Fig. 5 arise from a common lower state and the excitation probability into the continuum does not depend strongly on the excitation energy. From the fitted values of q and Γ listed in Table II, we estimate the transition probability into the upper state of feature B,

$$|\langle\Phi_B|T|i\rangle|^2 = |\langle\Phi_A|T|i\rangle|^2 \cdot \frac{q_A^2\Gamma_A}{q_B^2\Gamma_B}, \quad (7)$$

to be by a factor of 0.07 smaller than that of feature A. This observation supports the assignment of feature B to a $p-p$ type transition which is dipole-forbidden but mediated by the degenerate mode vibrational excitation. Such transitions from the $2p\ ^2A_2''(0,0,0,0)$ to the $3p\ ^2E'(0,1,1,0)$ and $3p\ ^2A_2''(0,1,1,0)$ levels were observed in the case of H_3 by Lembo *et al.*[15] The *np*-Rydberg series in H_3 was investigated by a two-photon excitation process via the $3s\ ^2A_1'(N=1,K=0)$ level.[17] The $N^+=1,K^+=0$ core excitation can be coupled with the *p*-electron to give A_2'' series with $N=0$ and $N=2$, and a E' series with $N=1$. Lembo *et al.*[17] observed a quantum defect of 0.05 ± 0.01 for the A_2'' series with $N=0$. This value agrees with that listed in Table III for a $(\nu_1=0, \nu_2=1)$ core excitation and supports our assignment of feature B in Fig. 5 to the $2p\ ^2A_2''(0,0,0,0) \rightarrow 8p\ ^2A_2''(0,1,1,0)$ transition.

D. Vibrational spacings of the $2p\ ^2A_2''$ state in D_3

A schematic diagram of the D_3 and D_3^+ states relevant for this investigation and the frequencies of the transitions assigned in the previous chapters is presented in Fig. 6. The separation between the $D_3^+(0,1,1,0)$ degenerate mode excited state and the (0,0,1,0) vibrational ground state of D_3^+ can be

TABLE III. Autoionization of core excited D_3 molecules.

D_3^+ vibration[a] $(\nu_1,\nu_2)^l$	Core energy[b] $E^+(\nu_1,\nu_2,1,0)$ (cm^{-1})	Autoionization[c] $\min(n-\delta)^c$	Peak A[d] n	Peak A[d] δ	Peak B[e] n	Peak B[e] δ
$(0,0)^0$	43.620					
$(0,1)^1$	1878.592	7.64	8	0.156	8	0.050
$(1,0)^0$	2343.677	6.84	7	0.014	8	0.939
$(0,2)^0$	3575.221	5.54	6	0.385	6	0.346
$(0,2)^2$	3694.866	5.45	6	0.479	6	0.442
$(1,1)^1$	4102.650	5.17	6	0.767	6	0.736
$(2,0)^0$	4595.870	4.89	5	0.062	5	0.036

[a]Core vibrational state labelled by $(\nu_1,\nu_2)^l$, ν_1=symmetric stretch, ν_2=degenerate mode, l=angular momentum associated with the degenerate mode.
[b]Energy $E^+(\nu_1,\nu_2,N^+=1,K^+=0)=E_v+2\cdot B_v$ of the $N^+=1,K^+=0$ rotationally excited ion core above the (0,0,0,0) state. Data taken from Amano *et al.*[35]
[c]Minimum required value of effective principal quantum number $n-\delta$ for vibrational autoionization of a Rydberg state with $(\nu_1,\nu_2)^l$ $(N^+=1,K^+=0)$ core excitation.
[d]Principal quantum number and quantum defect of feature A at 29652.6 cm^{-1} in the continuum assuming core vibrational excitation in column 1.
[e]Principal quantum number and quantum defect of feature B at 29700.7 cm^{-1} in the continuum assuming core vibrational excitation in column 1.

calculated to be $E^+(0,1,1,0)-E^+(0,0,1,0)=1834.972$ cm^{-1} from the values in Table III which are based on a direct spectroscopic investigation of the ν_2 series in D_3^+.[35] By combination of this value with the 29601.0 cm^{-1} limit of the $2p\ ^2A_2''(0,0,0,0)\rightarrow nd1(0,0,1,0)$-series and the 29535.1 cm^{-1} limit of the $2p\ ^2A_2''(0,1,0,0)\rightarrow nd1(0,1,1,0)$-series, we find the degenerate mode separation of the rotationless $2p\ ^2A_2''$ state to be 1900.9 cm^{-1}. We observed transitions from the $2p\ ^2A_2''(0,0,0,0)$ and the $2p\ ^2A_2''(1,0,0,0)$ states to the common upper state $7d1$ (1,0,1,0) at 27299.3 cm^{-1} and 29652.6 cm^{-1}, respectively. By combination of both frequencies, we find the symmetric stretch vibrational separation between the $2p\ ^2A_2''(0,0,0,0)$ and the $2p\ ^2A_2''(1,0,0,0)$ state of D_3 to be 2353.3 cm^{-1}. This value can be combined with the 29601.0 cm^{-1} limit of the $2p\ ^2A_2''(0,0,0,0)$ $\rightarrow nd1(0,0,1,0)$-series and the 29547.8 cm^{-1} limit of the $2p\ ^2A_2''(1,0,0,0)\rightarrow nd1(1,0,1,0)$-series (cf. table I). This places the separation between the $D_3^+(0,0,1,0)$ and $D_3^+(1,0,1,0)$ states at 2300.1 cm^{-1}. Our value is in excellent agreement with the difference $E^+(1,0,1,0)-E^+(0,0,1,0)$ = 2300.06 cm^{-1} calculated from the molecular constants by Amano *et al.*[35] which are based on the measured ν_2-sequence and the *ab initio* potential energy surface by Meyer, Botschwina and Burton (MBB).[38]

Our results for the vibrational constants of the $D_3\ 2p\ ^2A_2''(N=K=0)$ state are listed in Table IV. We be-

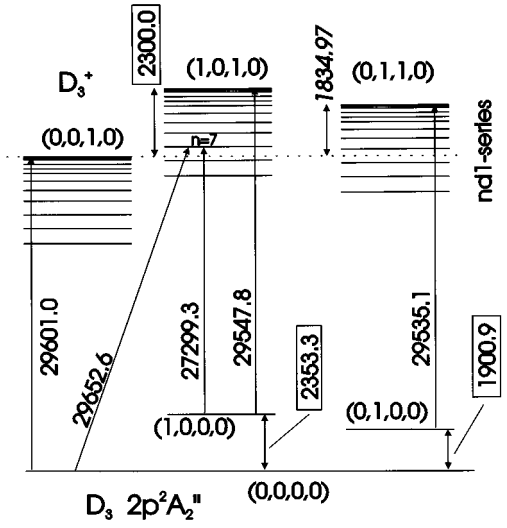

FIG. 6. Energy level scheme of the D_3 and D_3^+ molecule states relevant for the data presented in this paper. Observed transitions are indicated by single-arrow lines and labelled by the transition frequencies in cm^{-1}. The degenerate mode spacing of D_3^+ given in italics is calculated from the molecular constants by Amano *et al.*[35] The vibrational spacings deferred from the experimental results are enclosed in boxes.

TABLE IV. (a) Comparison of the vibrational separations in $D_3\ 2p\ ^2A_2''$, D_3^+, $H_3\ 2p\ ^2A_2''$, and H_3^+ molecules. (b) Ratio between vibrational frequencies in protonated and deuterated species. Upper numbers: ratios between the vibrational frequencies of the protonated and deuterated species; lower number: relative deviation of the upper number from the square-root of the mass ratio $r=\sqrt{m_d/m_p}=1.4138$ between deuterons (m_d) and protons (m_p).

$(\nu_1,\nu_2)^l$	$D_3\ 2p\ ^2A_2''$[a]	D_3^+[b]	ratio$_D$[c]	$H_3\ 2p\ ^2A_2''$[d]	H_3^+[e]	ratio$_H$[f]
$(0,1)^1$	1900.9	1834.674	1.0361	2618.34	2521.416	1.0384
$(1,0)^0$	2353.3	2300.843	1.0228	3255.38	3178.177	1.0243

$(\nu_1,\nu_2)^l$	b $2p\ ^2A_2''$	Ion
$(0,1)^1$	1.3774	1.3743
	-2.58×10^{-2}	-2.80×10^{-2}
$(1,0)^0$	1.3833	1.3813
	-2.16×10^{-2}	-2.30×10^{-2}

[a]This work.
[b]Amano *et al.*[35]
[c]Ratio$_D$: ratio between $D_3\ 2p\ ^2A_2''$ and D_3^+.
[d]Ketterle *et al.*[12]
[e]Majewski *et al.*[37]
[f]ratio$_H$: ratio between $H_3\ 2p\ ^2A_2''$ and H_3^+.

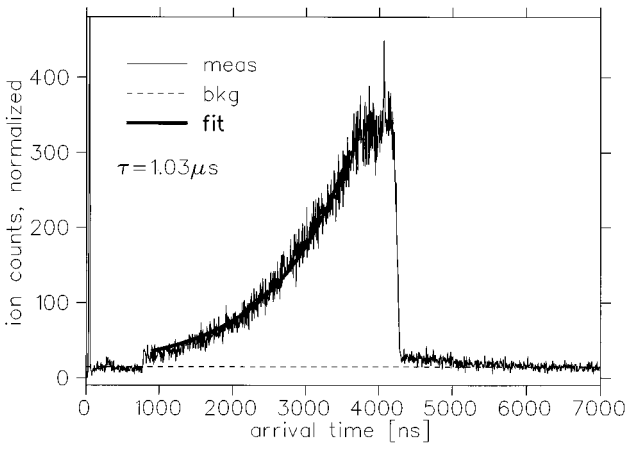

FIG. 7. Arrival time spectrum of the photoions with the laser exciting the transition from the D_3 $2p\ ^2A_2''(N=K=0)$ state into the continuum. The laser beam was expanded and collimated in order to produce a homogeneous beam profile over the entire length of the interaction region. The solid line is a single exponential fit to the measured spectrum between 900 ns and 3600 ns with a lifetime of $\tau = 1.03\ \mu$s.

lieve the experimental uncertainties to be of the order of 0.2 cm^{-1}. The values of the H_3 $2p\ ^2A_2''(N=K=0)$ molecule by Ketterle *et al.*,[12] the D_3^+ ion from Amano *et al.*,[35] and the H_3^+ ion by Majewski *et al.*[37] are included in Table IV for comparison. For the protonated as well as the deuterated species, the vibrational separations in the $2p\ ^2A_2''$ state of the neutral molecules are about 2% to 4% larger than those of the ion. This indicates that the $2p$ Rydberg electron increases the bond strength of the ion core. Interestingly, this increase is by 50% higher for the degenerate vibration mode than for the symmetric stretch vibration. The degenerate mode vibration is lower in energy and the vibrational wavefunction is localised closer to the origin where the effective charge distribution of the $2p$ orbital is higher.

The vibrational frequency ν of a particle of mass m moving in a pure harmonic potential is proportional to $1/\sqrt{m}$. In Table IV, the ratios between the corresponding vibrational frequencies of H_3 and D_3 in the $2p\ ^2A_2''$ state and of D_3^+ and H_3^+ are given. The values are slightly lower than the square-root of the mass-ratio $r=\sqrt{m_d/m_p}=1.4138$ for protons ($m_p = 1.00727u$) and deuterons ($m_d = 2.01355u$). The relative deviations from the ratio r are indicative of the anharmonicity of the potential and therefore are included in Table IV. The values are generally negative which means that the bond becomes softer with increasing energy of the vibrational state above the potential minimum. This effect is more pronounced for the degenerate mode vibration than for the symmetric stretch mode.

E. Lifetime of the $2p\ ^2A_2''$ state in D_3

In Fig. 7, the arrival-time spectrum of the photoions following laser-excitation of the $2p\ ^2A_2''$ metastables into the ionization continuum at 338.0 nm is presented. The resolution of the time-to-digital converter was 5 ns. Since the velocity of the neutrals is known, the time-of-flight can be mapped onto the position where the ions were created. The sharp peak at 50 ns is produced by scattered UV-photons from the laser pulse and marks the zeropoint of the timescale. A sharp step in the signal occurs at 800 ns. This amount of time is required for the photoions to travel from the entrance aperture of the quadrupole deflector to the microsphere plate detector. The modulations observed between 3600 ns and 4200 ns are produced by stray magnetic fields which distort the propagation of the photoions and thus reduce the collection efficiency in the detector. Photoions produced in the region between the charge transfer cell CT and the aperture (A in Fig. 1) are removed by the electric deflection field. This leads to the fast drop in signal for times greater than 4200 ns. The events above 6000 ns are not related to the laser pulse and are used to determine the background level. The range between 800 ns and 3600 ns corresponds to a comparatively field-free part of the laser-interaction region. In this range, the spectrum shows the exponential decay of the metastable density along the beam propagation. From a fit of a single exponential to the measurement, we find a decay time of $\tau = 1.03\ \mu$s. The fitted curve is indicated by the solid line in Fig. 7.

Due to the selected laser wavelength, the signal contains contributions from different vibrational states of the $2p\ ^2A_2''$ metastables. The measurements can be improved by exciting selected lines of the Rydberg series. This will be done in a separate investigation. The main contribution to the observed signal comes from ionization of the $2p\ ^2A_2''(0,0,0,0)$ state which constitutes the majority of the metastable beam. Systematic uncertainties arise from the finite laser beam and neutral beam divergences which affect the collection efficiency of the photoions as a function of the position on the beamline. We estimate the systematic uncertainty to be about $\pm 30\%$. The value of $\tau = 1.03\ \mu$s in D_3 is comparable in size to the 640 ns lifetime observed for the H_3 $2p\ ^2A_2''(N=K=0)$ state.[28] This may indicate that the lifetime of the metastable state in H_3 and D_3 is limited by the same decay mechanism which is most probably a vibrationally non-diagonal radiative transition onto the unstable ground state potential energy surface.[28,31]

IV. CONCLUSIONS

The metastability of the D_3 $2p\ ^2A_2''(N=K=0)$ state was demonstrated by two-photon resonance-enhanced photoionization via the $3d\ ^2E''(N=1, G=0, R=1)$ state. The lifetime of the $2p\ ^2A_2''(N=K=0)$ metastable state was estimated to be somewhat larger in D_3 than in H_3. Spectra of high principal quantum number Rydberg states were observed by field-ionization or autoionization following single-photon excitation in the ultraviolet spectral range. We observed *s*-type and *d*-type Rydberg series from vibrationally diagonal excitation of vibrational ground state, degenerate mode excited and symmetric stretch excited D_3 $2p\ ^2A_2''$ molecules. The ionization potential of the vibrationless $2p\ ^2A_2''(N=K=0)$ state was measured to be 29601.0 cm^{-1} by extrapolation of the Rydberg series. The existence of a $2p\ ^2A_2''(0,0,0,0) \rightarrow ns1(0,0,1,0)$ Rydberg series is surprising. This series was not observed in H_3 which shows that predis-

sociation is much weaker in D_3 than in H_3. Fano-type line profiles were observed in the continuum above the first ionization level of the $2p\ ^2A_2''(0,0,0,0)$ state and assigned to vibrationally non-diagonal transitions into $8p1(0,1,1,0)$ and $7d1(1,0,1,0)$ Rydberg states. By combination of vibrationally diagonal and non-diagonal transitions, and by comparison with spectroscopic data of D_3^+, we determined the lowest vibrational separations of the D_3 $2p\ ^2A_2''(N=K=0)$ molecule to be $\nu_1=2353.3\ \mathrm{cm}^{-1}$ and $\nu_2=1900.9\ \mathrm{cm}^{-1}$. By comparison between the vibrational separations in the $2p\ ^2A_2''$ metastable and the ionic state of H_3 and D_3, we find that the $2p\ ^2A_2''$ Rydberg electron increases the symmetric stretch mode frequency by 2% and the degenerate mode frequency by about 3.6%. Due to the anharmonicity of the potential energy surface, the ratios between the vibrational frequencies in H_3 and D_3 were found to deviate by about 2% from those of the harmonic oscillator.

ACKNOWLEDGMENTS

We are greatly indebted to Professor H. Helm (University of Freiburg) for his support and his continuous encouragement during the course of this work. Thanks must go to Professor R. Brenn for lending a multistop time-to-digital converter to us. We wish to thank Dr. G. Alber (University of Freiburg) for fruitful discussions concerning the Fano profiles. It is a pleasure to acknowledge technical assistance by U. Person (University of Freiburg) during the construction and operation of the apparatus. This research was financially supported by Deutsche Forschungsgemeinschaft (SFB 276, TP C13).

[1] I. Dabrowski and G. Herzberg, Can. J. Phys. **58**, 1238 (1980).
[2] G. Herzberg and J. K. G. Watson, Can. J. Phys. **58**, 1250 (1980).
[3] G. Herzberg, H. Lew, J. J. Sloan, and J. K. G. Watson, Can. J. Phys. **59**, 428 (1981).
[4] G. Herzberg, J. T. Hougen, and J. K. G. Watson, Can. J. Phys. **60**, 1261 (1982).
[5] F. M. Devienne, C. R. Acad. Sci. Paris B **267**, 1279 (1968); and **268**, 1303 (1969).
[6] G. I. Gellene and R. F. Porter, J. Chem. Phys. **79**, 5975 (1983).
[7] J. F. Garvey and A. Kuppermann, Chem. Phys. Lett. **107**, 491 (1984).
[8] H. Helm, L. J. Lembo, P. C. Cosby, and D. L. Huestis, *Fundamentals of Laser Interactions II*, Lecture Notes in Physics, edited by F. Ehlotzky, (Springer–Verlag, Berlin, 1989), p. 264.
[9] H. Helm, Phys. Rev. Lett. **56**, 42 (1986).
[10] H. Helm, Phys. Rev. A **38**, 3425 (1988).
[11] A. Dodhy, W. Ketterle, H.-P. Messmer, and H. Walther, Chem. Phys. Lett. **151**, 133 (1988).
[12] W. Ketterle, H.-P. Messmer, and H. Walther, Europhys. Lett. **8**, 333 (1989).
[13] L. J. Lembo, A. Petit, and H. Helm, Phys. Rev. A **39**, 3721 (1989).
[14] L. J. Lembo and H. Helm, Chem. Phys. Lett. **163**, 425 (1989).
[15] L. J. Lembo, D. Huestis, and H. Helm, J. Chem. Phys. **90**, 5299 (1989).
[16] L. J. Lembo, M. C. Bordas, and H. Helm, Phys. Rev. A **42**, 6660 (1990).
[17] M. C. Bordas, L. J. Lembo, and H. Helm, Phys. Rev. A **44**, 1817 (1991).
[18] H. Helm, in *Dissociative Recombination*, edited by B. R. Rowe (Plenum, New York, 1993), p. 145; Phys. Rev. A **44**, 1817 (1991).
[19] Z. Peng, S. Kristyan, A. Kuppermann, and J. S. Wright, Phys. Rev. A. **52**, 1005 (1995).
[20] H. Figger, W. Ketterle, and H. Walther, Z. Phys. D **13**, 129 (1989).
[21] W. Ketterle, H. Figger, and H. Walther, Z. Phys. D **13**, 139 (1989).
[22] B. Barbieri, N. Beverini, and A. Sasso, Rev. Mod. Phys **62**, 603 (1990).
[23] *MIT Wavelength Tables* (Harrison, Cambridge, 1969).
[24] D. H. Rank, in *Advances in Spectroscopy I*, edited by H. W. Thompson (Interscience, New York, 1959).
[25] C. E. Moore, *Atomic Energy Levels*, Circular of the NBS 467 (U. S. Government Printing Office, Washington DC, 1948), Vol. I, p. 1.
[26] H. F. King and K. Morokuma, J. Chem. Phys. **71**, 3213 (1979).
[27] I. D. Petsalakis, G. Theodorakopoulos, and J. S. Wright, J. Chem. Phys. **89**, 6850 (1988).
[28] C. Bordas, P. C. Cosby, and H. Helm, J. Chem. Phys. **93**, 6303 (1990).
[29] N. Bjerre, I. Hazell, and D. C. Lorents, Chem. Phys. Lett. **181**, 301 (1991).
[30] P. C. Cosby and H. Helm, Phys. Rev. Lett. **61**, 298 (1988).
[31] U. Müller and P. C. Cosby, J. Chem Phys. **105**, 3532 (1996).
[32] J. K. G. Watson, S. C. Foster, A. R. W. McKellar, P. Bernath, T. Amano, F. S. Pan, M. W. Crofton, R. S. Altman, and T. Oka, Can. J. Phys. **62**, 1875 (1984).
[33] H. Figger, Y. Fukuda, W. Ketterle, and H. Walther, Can. J. Phys. **62**, 1274 (1984).
[34] G. Herzberg, *Molecular Spectra and Molecular Structure III*, Electronic Spectra of and Electronic Structure of Polyatomic Molecules (Van Nostrand Reinhold, New York, 1966).
[35] T. Amano, M.-C. Chan, S. Civis., A. R. W. McKellar, W. A. Majewski, D. Sadovskii, and J. K. G. Watson, Can. J. Phys. **72**, 1007 (1994).
[36] H. A. Bethe and E. E. Salpeter, *Quantum Mechanics of One- and Two-Electron Atoms* (Plenum, New York, 1977).
[37] W. A. Majewski, A. R. W. McKellar, D. Sadovskii, and J. K. G. Watson, Can. J. Phys. **72**, 1016 (1994).
[38] W. Meyer, P. Botschwina, and P. Burton, J. Chem. Phys. **84**, 891 (1986).
[39] U. Fano, Phys. Rev. **124**, 1866 (1961).
[40] W. Ketterle, H.-P. Messmer, and H. Walther, Europhys. Lett. **8**, 333 (1989).